Development 140, 2118-2129 (2013) doi:10.1242/dev.092833

Arabidopsis HD-Zip II transcription factors control apical embryo development and meristem function

Luana Turchi[1,*], Monica Carabelli[1,*], Valentino Ruzza[1], Marco Possenti[2], Massimiliano Sassi[1,‡], Andrés Peñalosa[2], Giovanna Sessa[1], Sergio Salvi[2], Valentina Forte[2], Giorgio Morelli[2] and Ida Ruberti[1,§]

SUMMARY

The *Arabidopsis* genome encodes ten Homeodomain-Leucine zipper (HD-Zip) II proteins. *ARABIDOPSIS THALIANA HOMEOBOX 2* (*ATHB2*), *HOMEOBOX ARABIDOPSIS THALIANA 1* (*HAT1*), *HAT2*, *HAT3* and *ATHB4* are regulated by changes in the red/far red light ratio that induce shade avoidance in most of the angiosperms. Here, we show that progressive loss of HAT3, ATHB4 and ATHB2 activity causes developmental defects from embryogenesis onwards in white light. Cotyledon development and number are altered in *hat3 athb4* embryos, and these defects correlate with changes in auxin distribution and response. *athb2* gain-of-function mutation and ATHB2 expression driven by its promoter in *hat3 athb4* result in significant attenuation of phenotypes, thus demonstrating that ATHB2 is functionally redundant to HAT3 and ATHB4. In analogy to loss-of-function mutations in HD-Zip III genes, loss of HAT3 and ATHB4 results in organ polarity defects, whereas triple *hat3 athb4 athb2* mutants develop one or two radialized cotyledons and lack an active shoot apical meristem (SAM). Consistent with overlapping expression pattern of HD-Zip II and HD-Zip III gene family members, bilateral symmetry and SAM defects are enhanced when *hat3 athb4* is combined with mutations in *PHABULOSA* (*PHB*), *PHAVOLUTA* (*PHV*) or *REVOLUTA* (*REV*). Finally, we show that *ATHB2* is part of a complex regulatory circuit directly involving both HD-Zip II and HD-Zip III proteins. Taken together, our study provides evidence that a genetic system consisting of HD-Zip II and HD-Zip III genes cooperates in establishing bilateral symmetry and patterning along the adaxial-abaxial axis in the embryo as well as in controlling SAM activity.

KEY WORDS: Auxin, Embryo bilateral symmetry, Cotyledon development, Shoot apical meristem activity, HD-Zip III transcription factors, *Arabidopsis*

INTRODUCTION

In plants, as in animals, the basic body plan is laid down during embryogenesis. This begins with an asymmetric cell division of the zygote that gives rise to a larger basal cell and a smaller apical cell. The basal cell and its derivatives repeatedly divide horizontally forming a filamentous suspensor, which connects the embryo with the maternal tissue. The uppermost suspensor cell is subsequently recruited by the embryo and specified to become the hypophysis, the founder of the root apical meristem (RAM). The apical cell and its derivatives undergo a series of highly coordinated divisions to form a globular embryo proper. During embryo development, formation of the apical-basal axis is followed by establishment of the radial axis and finally of bilateral symmetry. The SAM forms between the two out-growing cotyledons from the globular stage onwards (De Smet et al., 2010).

The *Arabidopsis* embryo has been widely used for studying patterning events in plants by virtue of the nearly invariant cell division pattern during early embryogenesis, and in recent years a number of factors underpinning the establishment of a basic body plan have been identified (De Smet et al., 2010; Zhao et al., 2011; Lau et al., 2012).

Auxin plays a prominent role in *Arabidopsis* embryo development, and an ever-increasing body of evidence shows that auxin biosynthesis, transport and response are all crucial for pattern formation (Möller and Weijers, 2009). Directional transport of auxin is determined by the asymmetric membrane localization of the efflux carriers, the PIN-FORMED (PIN) family of proteins (Wisniewska et al., 2006). At least four PINs – PIN1, PIN3, PIN4, PIN7 – are dynamically expressed during embryogenesis, and quadruple mutants of all four genes exhibit severe embryonic phenotypes, including embryos lacking apical-basal polarity (Friml et al., 2003; Blilou et al., 2005; Vieten et al., 2005). Mutations in genes regulating PIN protein localization, which depends on trafficking, recycling, degradation and reversible phosphorylation, result in abnormal auxin distribution and defects in embryo patterning (Möller and Weijers, 2009; De Smet et al., 2010; Zhao et al., 2011). Auxin-induced gene expression involves activation of AUXIN RESPONSE FACTORS (ARFs), transcription factors that activate or repress target genes (Guilfoyle and Hagen, 2007). ARFs are negatively regulated by AUXIN/INDOLE-3-ACETIC ACID (AUX/IAA) proteins, which are targeted for degradation in response to auxin (Gray et al., 2001; Santner et al., 2009). Mutations in *MONOPTEROS* (*MP*) (also known as *ARF5*) result in defects in both apical and basal patterning processes. MP is required for hypophysis specification, and *mp* mutants exhibit a rootless phenotype (Berleth and Jürgens, 1993; Weijers et al., 2006); gain-of-function mutations in BODENLOS (BDL) (also known as IAA12), which binds to MP and inhibits its activity, result in the same phenotype (Hamann et al., 2002). In addition, *mp* and *bdl* exhibit cotyledon formation defects (Berleth and Jürgens, 1993; Hamann et al., 2002). MP directly activates the expression of the AP2 transcription factor gene *DORNRÖSCHEN* (*DRN*) in the tips

[1]Institute of Molecular Biology and Pathology, National Research Council, P.le A. Moro 5, 00185 Rome, Italy. [2]National Research Institute on Food and Nutrition, Via Ardeatina 546, 00178 Rome, Italy.

*These authors contributed equally to this work
‡Present address: Laboratoire de Reproduction et Développement des Plantes, École Normale Supérieure de Lyon 46, Allée d'Italie, 69364 Lyon, CEDEX 07, France
§Author for correspondence (ida.ruberti@uniroma1.it)

Accepted 18 February 2013

of the embryonic cotyledons. DRN acts redundantly with its paralog DRN-like (DRNL) in cotyledon development, and different lines of evidence indicate that it might control auxin transport (Chandler et al., 2007; Cole et al., 2009).

Proper patterning of the apical region of the globular embryo requires the activity of members of the HD-Zip III protein family (Emery et al., 2003; Prigge et al., 2005). This family consists of five genes – *PHB*, *PHV*, *REV*, *ATHB8* and *ATHB15* [also known as *CORONA* (*CNA*) and *INCURVATA 4* (*ICU4*)] – all predicted to be regulated by miR 165 and miR 166 (Emery et al., 2003; Floyd and Bowman, 2004; Mallory et al., 2004). The *phb rev* double, *phb phv rev* triple and other mutant combinations involving *athb8* and *athb15* lack the SAM and, in most severe cases, fail to establish bilateral symmetry (Emery et al., 2003; Prigge et al., 2005). Defects in the pattern of PIN1 expression are evident in *phb phv rev* embryos at the heart stage (Izhaki and Bowman, 2007). Several recent findings further support a key role for HD-Zip III proteins in apical embryo development. First, failure to restrict HD-Zip III expression in the apical domain via a miRNA-dependent pathway prevents proper establishment of the embryonic root pole (Grigg et al., 2009). Second, semi-dominant gain-of-function mutations in the miR-binding site of *PHB*, *REV* and *ICU4* restore the *tpl1-1* double-root phenotype, possibly by excluding PLETHORA 1 (PLT1) and PLT2, master regulators of root development expression of which partially depends on MP activity (Aida et al., 2004; Blilou et al., 2005; Galinha et al., 2007), from the embryo apical domain (Long et al., 2006; Smith and Long, 2010). Finally, mis-expression of miR 165- and miR 166-resistant variants of *REV*, *PHB* or *ICU4* in the basal cells of the embryo produces a transformation of the root pole into a second shoot pole, indicating that HD-Zip III proteins act as master regulators of embryonic apical fate (Smith and Long, 2010).

The HD-Zip III genes are also involved in patterning along the radial and adaxial-abaxial axes of the embryo. *PHB*, *PHV* and *REV* are all expressed in the apical half of globular embryos. Later in embryogenesis, expression is restricted to the SAM, the adaxial region of the cotyledons and the provasculature (McConnell et al., 2001; Emery et al., 2003). *phb phv rev* mutants frequently form a single abaxialized radial cotyledon with vascular bundles showing amphicribal symmetry and lack the SAM (Emery et al., 2003). A key role for PHB, PHV and REV in radial patterning throughout plant development has also been demonstrated (McConnell and Barton, 1998; McConnell et al., 2001; Emery et al., 2003; Zhong and Ye, 2004; Prigge et al., 2005).

Here, we show that members of the HD-Zip II protein family, mostly known for their role in shade avoidance (Ruberti et al., 2012), and recently implicated in carpel margin development (Reymond et al., 2012) and leaf polarity (Bou-Torrent et al., 2012), also control embryonic apical patterning and SAM function at least in part through interaction with HD-Zip III proteins.

MATERIALS AND METHODS

Plant lines and growth

Wild type (wt): *Arabidopsis thaliana* (L.) Heynh var. Columbia (Col-0). Insertional lines: *athb2-1* (Salk_106790) (Khanna et al., 2006), *athb2-2* (Salk_006502), *athb2-3* (Babiychuk et al., 1997), *athb4-1* (Salk_104843) (Sorin et al., 2009), *athb4-3* (Sussman et al., 2000), *hat3-2* (GT5653), *hat3-3* (Salk_014055), *phb-13* (Salk_021684) (Prigge et al., 2005), *phv-11* (SalkJP91_0F10L.47.75) (Prigge et al., 2005), *rev-5* (Talbert et al., 1995). Gene trap lines: *hat3-4* (GT9206; Cold Spring Harbor collection), which carries a gene-trap Ds insertion within *HAT3* (HAT3::GUS) (Nakayama et al., 2005) at nucleotide +194 from the ATG, *yab3-2* (Kumaran et al., 2002). Insertional lines and gene trap lines were identified by PCR genotyping (see supplementary material Table S1 for primer details). The *rev-5* allele was identified by dCAPS method: genomic DNA was amplified with primers rev-5 up and rev-5 down (see supplementary material Table S1 for primer details), then cut with *Rsa*I. Restriction fragments were separated on a 2% agarose gel. The *athb2-3* line, which was originally in the *Arabidopsis* C24 background (Babiychuk et al., 1997), was backcrossed five times to Col-0 prior to any phenotypic analysis and to any cross with other lines. Plants were grown in white light as described (Steindler et al., 1999). For NPA experiments, seeds were germinated and grown for 7 days on agar plates containing either 10 μM 1-naphthylphthalamic acid (NPA) dissolved in DMSO, or DMSO alone.

Genetic analysis

HD-Zip II double mutants: *hat3-3 athb4-1*, *hat3-3 athb4-3*, *hat3-2 athb4-1*, *hat3-3 athb2-1*, *hat3-3 athb2-3*, *athb4-1 athb2-1*, *athb4-1 athb2-3*. *hat3-3 athb4-1*, *hat3-3 athb4-3* and *hat3-2 athb4-1* were selected in F_2 by phenotyping and PCR genotyping, and re-analyzed in F_3. *hat3-3 athb2-1*, *hat3-3 athb2-3*, *athb4-1 athb2-1* and *athb4-1 athb2-3* mutants were selected in F_2 and re-analyzed in F_3 by PCR genotyping (see supplementary material Table S1 for primer details). Higher order HD-Zip II mutants: *hat3-3 athb4-1 athb2-1*, *hat3-3 athb4-1 athb2-2*, *hat3-3 athb4-1 athb2-3*. *hat3-3 athb4-1 athb2-1* and *hat3-3 athb4-1 athb2-3* triple mutants, selected in F_2 by phenotyping and PCR genotyping, growth arrested at the seedling stage either on agar plate (*hat3-3 athb4-1 athb2-1*, n=70; *hat3-3 athb4-1 athb2-3*, n=83) and on soil (*hat3-3 athb4-1 athb2-1*, n=71; *hat3-3 athb4-1 athb2-3*, n=79). Therefore, *hat3-3/+ athb4-1 athb2-1* and *hat3-3/+ athb4-1 athb2-3* were selected in F_2 by genotyping and propagated. HD-Zip II/HD-Zip III combinations: *hat3-3 phv-11*, *athb4-1 phv-11*, *hat3-3/+ athb4-1 phv-11*, *hat3-3 phb-13*, *athb4-1 phb-13*, *hat3-3 athb4-1/+ phb-13*, *hat3-3 rev-5*, *athb4-1 rev-5*, *hat3-3 athb4-1/+ rev-5*. All the alleles with the exception of *rev-5* were identified by PCR genotyping. The *rev-5* allele was identified by dCAPS (see supplementary material Table S1 for primer details). A 2×2 contingency table followed by Fisher's exact test was used to compare the frequency of occurrence of phenotype in double or triple homozygous and other genotypes except double or triple homozygous groups. Markers were introduced in *hat3-3 athb4-1* by crossing. *hat3-3 athb4-1* plants were selected by phenotyping and genotyping. Homozygosity of all the reporters, with the exception of YAB3::GUS, was determined by unanimous GUS and GFP signal (n≥30). For YAB3::GUS, a segregating *hat3-3 athb4-1* YAB3::GUS/+ was identified.

Gene constructs and transformation

DNA constructs: HAT3::HAT3:GFP, ATHB2::ATHB2:GUS, ATHB4::GUS, 35S::HAT3:GFP, XVE::HAT3, 35S::3HA:ATHB2, 35S::ATHB2:GFP, XVE::ATHB8d. Primers used to generate all the constructs are listed in supplementary material Table S1. Col-0 plants were transformed as described (Steindler et al., 1999). HAT3::HAT3:GFP and ATHB2::ATHB2:GUS were also stably transferred in *hat3-3 athb4-1*. Double mutants were selected by genotyping and homozygosity of HAT3::HAT3:GFP and ATHB2::ATHB2:GUS was determined by unanimous GFP and GUS signal (n≥30).

In situ hybridization and GUS analysis

In situ hybridizations were detected with digoxigenin-labeled riboprobes using the method described by Hejátko et al. (Hejátko et al., 2006) with minor modifications. *HAT3*, *ATHB4* and *ATHB2* probes were generated using full-length cDNAs. GUS analyses were performed as described (Carabelli et al., 2007).

Chromatin immunoprecipitation (ChIP)

Whole seedlings were fixed and nuclei were prepared according to the manufacturer's instructions using the CelLytic PN Kit (Sigma). ChIP was performed as described by Zhao et al. (Zhao et al., 2010) with minor modifications. Chromatin was solubilized with a Misonix S-4000 Cuphorn [10 seconds on/15 seconds off for 24 minutes, using recirculating chilling water flux (8-10°C), amplitude 60], and immunoprecipitated with anti-GFP (ab290-50, Abcam, UK). A negative control was performed, including a ChIP reaction performed on wt.

Real-time PCR

For gene expression analysis, mRNA purification, cDNA synthesis and quantitative real-time PCR (qPCR) were performed as described (Ciarbelli et al., 2008). For ChIP samples, qPCR was performed with the SYBR Green PCR Master Mix (Applied Biosystems, USA) using the ABI Prism 7900HT Sequence Detection System (Applied Biosystems, USA) according to the manufacturer's instructions. Each amplification was performed in triplicate using a primer concentration of 400 nM. Primers: ATHB2_A_Fwd (HAT4-IF) (Brandt et al., 2012), ATHB2_A_Rvs (HAT4-IR) (Brandt et al., 2012), ATHB2_B_Fwd, ATHB2_B_Rvs, ATHB2_C_Fwd, ATHB2_C_Rvs, LAX3_N_Fwd, LAX3_N_Rvs (supplementary material Table S1). Fold enrichment was determined by comparing the CT (threshold cycle) values of immunoprecipitated (IP) and negative control which were normalized by calculating input(IP)/input(control).

Phenotype analysis and microscopy

For vascular pattern analysis, samples were analyzed as described (Carabelli et al., 2007). For differential interference contrast (DIC) analysis of embryos, ovules were cleared in chloral hydrate (Weigel and Glazebrook, 2002), mounted on slides and viewed under Axioskop 2 plus binocular microscope (Zeiss, Germany). Sections were performed as described by Steindler et al. (Steindler et al., 1999). Means were compared using *t*-test analysis. Phenotypic distributions were compared using a contingency table followed by Fisher's exact test.

Confocal microscopy

Confocal microscopy analyses were performed on Inverted Z.1 microscope (Zeiss, Germany) equipped with Zeiss LSM 700 spectral confocal laser scanning unit (Zeiss, Germany). Samples were excited with a 488 nm, 10 mW solid laser with emission at 492-539 nm. Embryos were dissected from ovules and fixed under vacuum for 30 minutes in 4% paraformaldehyde. Samples were washed twice in PBS and mounted in 50% glycerol.

RESULTS

hat3 athb4 mutants display defects in cotyledon number and development

The *Arabidopsis* genome contains ten HD-Zip II genes, five of which regulated by light quality changes (γ clade: *HAT1*, *HAT2*, *ATHB2*; δ clade: *HAT3*, *ATHB4*) (Ciarbelli et al., 2008). To address the function of HD-Zip IIδ genes, we characterized *hat3* (*hat3-2*, *hat3-3*) and *athb4* (*athb4-1*, *athb4-3*) insertional lines. All *hat3* and *athb4* alleles are likely to represent loss-of-function mutants (supplementary material Fig. S1A-D). Single mutants show no obvious morphological defect in white light (supplementary material Fig. S2). However, seedlings with altered cotyledons segregated with the ratio expected for two independent and recessive mutations in the F_2 of the crosses between *hat3* and *athb4*. Phenotype/genotype co-segregation analyses demonstrated that cotyledon alteration is associated with the *hat3* and *athb4* mutations (supplementary material Fig. S3 and Tables S2-S5).

In all double mutants characterized the cotyledon phenotype displays variable expressivity. *hat3 athb4* seedlings show varying degrees of cotyledon expansion, from round-shaped to almost completely radialized organs. Furthermore, seedlings with fused/single cotyledon(s) were often found among the *hat3 athb4* mutants ($P<0.0001$). The pattern of vascular development is also profoundly altered in *hat3 athb4* cotyledons, and the defects correlate with the severity of the expansion phenotype. For example, fully radialized cotyledons have no recognizable vasculature (supplementary material Fig. S4). The *hat3 athb4* cotyledon phenotype was almost completely rescued by introducing the wt *HAT3* gene in the double mutant (supplementary material Figs S5, S6).

HAT3 and *ATHB4* are co-expressed during embryogenesis

The double mutant phenotypes imply that HAT3 and ATHB4 are required for proper embryo patterning. Consistent with this, *in situ* hybridization revealed specific expression patterns of *HAT3* and *ATHB4* during embryogenesis (Fig. 1; supplementary material Fig. S7). At the early globular stage, *HAT3* is expressed in the embryo proper and excluded from the hypophysis. By the heart stage, the expression domain of *HAT3* is mostly restricted to the apical part of the embryo, marking the incipient cotyledons. At the torpedo stage, *HAT3* is mainly expressed in the adaxial side of the cotyledons and in the SAM. In mature embryos, *HAT3* marks the SAM and the provascular system (Fig. 1A-E). *ATHB4* is mainly expressed in the apical domain of globular and transition stage embryos. By the heart stage, *ATHB4* expression resembles that of *HAT3* (Fig. 1F-J).

Auxin distribution and response are altered in *hat3 athb4* embryos

hat3-3 athb4-1 plants are profoundly altered throughout development and produce few seeds (data not shown). Therefore, to gain insights into the role of the HD-Zip IIδ proteins in the early stages of development, mature embryos were isolated from *hat3-3 athb4-1*/+ plants. Embryos with altered cotyledons segregated with the ratio expected for a single recessive mutation. As expected, embryos with fused/single cotyledon(s) were observed. The remaining altered embryos display, as observed in *hat3-3 athb4-1* seedlings, varying degrees of defects in cotyledon development (supplementary material Fig. S8).

Auxin has a key role in both initiation and development of cotyledons during embryogenesis (Chandler, 2008). To investigate whether HAT3 and ATHB4 interfere with auxin distribution and response, *hat3-3 athb4-1* was crossed with DR5rev::GFP (Friml et al., 2003). Mature embryos with two cotyledons differing in their

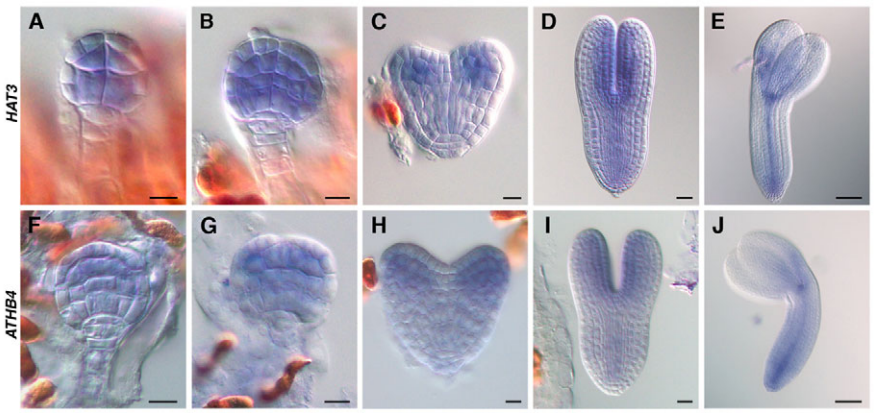

Fig. 1. *HAT3* and *ATHB4* expression during embryogenesis. (**A-J**) *In situ* hybridization with *HAT3* (A-E) and *ATHB4* (F-J) probes. Globular (A,F), transition (B,G), heart (C,H), torpedo (D,I) and mature (E,J) embryos. Scale bars: A-C,F-H, 5 μm; D,I, 10 μm; E,J, 50 μm.

degree of expansion and those with fused/single cotyledon(s) were selected to determine DR5rev::GFP pattern. Among the former, consistent with the phenotypes observed in *hat3-3 athb4-1* seedlings, the most frequently seen were those with one cotyledon moderately expanded and one more significantly impaired in expansion (Fig. 2E,F; supplementary material Fig. S4A; data not shown). No significant difference was observed in DR5rev::GFP maximum in the root tip in *hat3-3 athb4-1* embryos relative to Col-0. By contrast, GFP signal was significantly reduced or almost undetectable in cotyledons of mutant embryos (Fig. 2C,G). Remarkably, DR5rev::GFP expression strictly correlated with the degree of cotyledon expansion (Fig. 2G; data not shown). A significant number of *hat3-3 athb4-1* seedlings displayed fused/single cotyledon(s) (Fig. 2I,J,M,N; supplementary material Fig. S4A). *hat3-3 athb4-1* embryos with fused/single expanded cotyledon(s) display either two very close DR5rev::GFP maxima (Fig. 2K) or a single DR5rev::GFP maximum (Fig. 2O).

To investigate further the links between auxin response and distribution and HAT3 and ATHB4 function, *hat3-3 athb4-1* was crossed with PIN1::PIN1:GFP (Benková et al., 2003). Remarkably, PIN1:GFP expression in mature mutant embryos (Fig. 2H,L,P) closely mirrors the vascular defects observed in *hat3-3 athb4-1* seedlings (Fig. 2F,J,N; supplementary material Fig. S4A). No significant difference was observed in PIN1:GFP expression in hypocotyls and roots of embryos altered in cotyledon development relative to wt (Fig. 2D,H,L,P).

athb2 loss-of-function mutations enhance *hat3 athb4* defects in cotyledon number and development

The incomplete expressivity of the *hat3 athb4* phenotype suggests functional redundancy within the HD-Zip II protein family. The genes most closely related to *HAT3* and *ATHB4* are *HAT1*, *HAT2* and *ATHB2*, all belonging to clade γ (Ciarbelli et al., 2008). *HAT1* and *HAT2* are paralogous genes, and, therefore, *ATHB2* was chosen to investigate redundancy between HD-Zip IIγ and HD-Zip IIδ genes.

In situ hybridization revealed specific expression pattern of *ATHB2* during embryogenesis (Fig. 3A-C; supplementary material Fig. S7). At the globular stage, *ATHB2* is expressed in the procambial cells. The vascular expression is maintained throughout all developmental stages. By the late torpedo stage until maturation, *ATHB2* is also expressed in RAM. A weak expression of *ATHB2* is also detected in SAM of mature embryos (Fig. 3A-C).

To investigate *ATHB2* function, we characterized *athb2* insertional lines. *athb2-1* and *athb2-3* are likely to represent loss-of-function mutants whereas *athb2-2* is a gain-of-function mutant (supplementary material Fig. S1E-G). *athb2-1* and *athb2-3* show no obvious morphological defect in white light whereas *athb2-2* seedlings display slightly elongated hypocotyls and smaller cotyledons. Lack of ATHB2 in *hat3-3* and *athb4-1* does not result in any major phenotype in white light (supplementary material Fig. S2). We then isolated and characterized *hat3-3/+ athb4-1 athb2-1* and *hat3-3/+ athb4-1 athb2-3* lines (supplementary material Tables S6, S7). The phenotype of *hat3-3 athb4-1 athb2-1* and *hat3-3 athb4-1 athb2-3* is significantly more severe than that of *hat3-3 athb4-1*. Remarkably, almost all triple mutants display radialized cotyledons. Moreover, the number of seedlings with fused/single cotyledon(s) is significantly higher in the *hat3-3 athb4-1 athb2-1* and *hat3-3 athb4-1 athb2-3* populations than in the *hat3-3 athb4-1* one (Fig. 3G,H; supplementary material Fig. S9 and Table S8).

athb2 gain-of-function mutation and ATHB2:GUS expression attenuate *hat3 athb4* defects in cotyledon organogenesis

To gain further insights into the relationships between *ATHB2* and HD-Zip IIδ genes, we took advantage of the *athb2-2* gain-of-

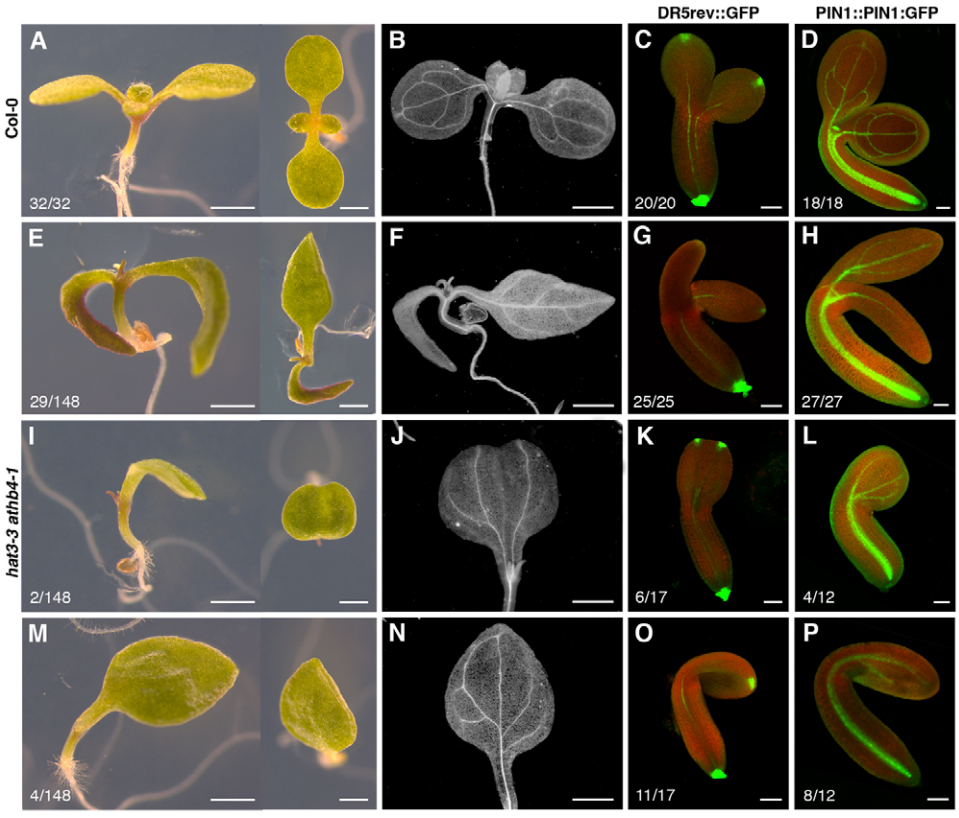

Fig. 2. *hat3 athb4* embryos display altered expression of DR5rev::GFP and PIN1::PIN1:GFP. (**A-P**) Col-0 (A) and *hat3-3 athb4-1* (E,I,M) seedlings and dark-field images of the same seedlings (B,F,J,N), and fluorescent images of DR5rev::GFP (C), *hat3-3 athb4-1* DR5rev::GFP (G,K,O), PIN1::PIN1:GFP (D) and *hat3-3 athb4-1* PIN1::PIN1:GFP (H,L,P) embryos. Scale bars: A,B,E,F,I,J,M,N, 1 mm; C,D,G,H,K,L,O,P, 50 µm.

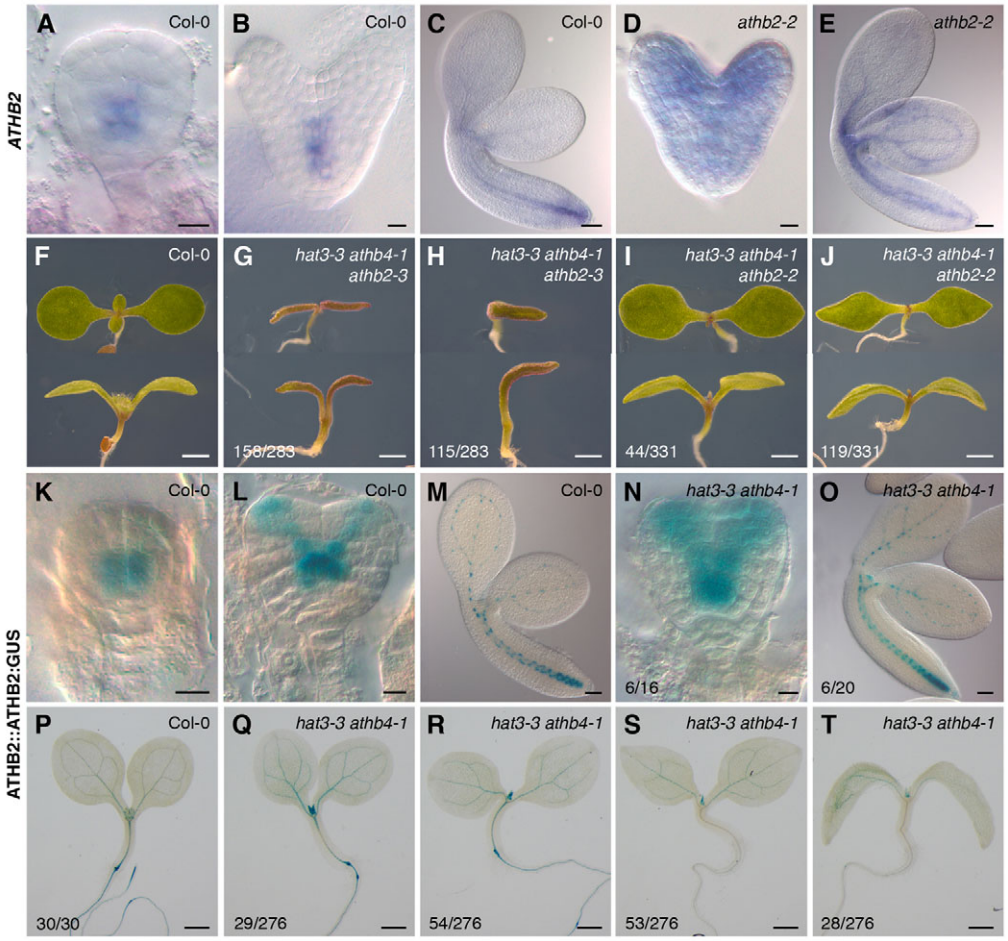

Fig. 3. ATHB2 is redundant to HAT3 and ATHB4 in regulating embryo bilateral symmetry and cotyledon development. (**A-E**) *In situ* hybridization of Col-0 (A-C) and *athb2-2* (D,E) embryos with *ATHB2* probe. (**F-J**) Col-0 (F), *hat3-3 athb4-1 athb2-3* (G,H) and *hat3-3 athb4-1 athb2-2* (I,J) seedlings. (**K-T**) GUS localization in ATHB2::ATHB2:GUS (K-M,P) and *hat3-3 athb4-1* ATHB2::ATHB2:GUS (N,O,Q-T) embryos (K-O) and seedlings (P-T). Scale bars: A,B,D,K,L,N, 10 μm; C,E,M,O, 50 μm; F-J, 1 mm; P-T, 0.5 mm.

function mutant. *In situ* hybridization in *athb2-2* embryos revealed the presence of *ATHB2* transcript not only in the provascular cells, as observed in wt, but also in the adaxial side of incipient cotyledons (Fig. 3B,D) where *HAT3* and *ATHB4* are expressed. Moreover, increased levels of *ATHB2* were detected in vascular cells and in SAM of *athb2-2* mature embryos relative to wt (Fig. 3C,E). Remarkably, *athb2-2* significantly attenuates the *hat3-3 athb4-1* cotyledon development phenotype (Fig. 3I,J; supplementary material Fig. S10 and Table S9). However, no significant difference was observed in cotyledon number between *hat3-3 athb4-1* and *hat3-3 athb4-1 athb2-2* (P=0.54).

To analyze the expression pattern of ATHB2 in *hat3-3 athb4-1*, ATHB2::ATHB2:GUS chimeric gene was constructed (supplementary material Fig. S5). In wt embryos, ATHB2:GUS is localized in provascular cells from the early globular stage throughout all developmental stages (Fig. 3K-M), as *ATHB2* RNA. There are, however, some differences in ATHB2:GUS expression pattern compared with that of *ATHB2*. Weak expression of ATHB2:GUS was detected in the apical side of heart embryos, but no GUS signal was seen in SAM at late stages of embryo development (Fig. 3L,M). This might be due to the absence of one or more regulatory elements in the chimeric gene or might be the consequence of additional regulation at the translational and/or post-translational level. Interestingly, ATHB2:GUS expression was enhanced in the apical side of early heart *hat3-3 athb4-1* embryos with respect to wild-type ones (Fig. 3L,N; P=0.0002). Furthermore, ATHB2:GUS was also detected in SAM of several *hat3-3 athb4-1* mature embryos (Fig. 3O). To evaluate whether the increase of ATHB2 expression in *hat3-3 athb4-1* is functionally relevant, *hat3-3 athb4-1* ATHB2::ATHB2:GUS seedlings were phenotypically analyzed. Remarkably, the phenotype of *hat3-3 athb4-1* ATHB2::ATHB2:GUS was significantly less severe than that of *hat3-3 athb4-1*. Most of the *hat3-3 athb4-1* ATHB2::ATHB2:GUS seedlings display round and lancet cotyledons (Fig. 3R,S). Moreover, ~10% of *hat3-3 athb4-1* ATHB2::ATHB2:GUS seedlings show a completely rescued phenotype characterized by round cotyledons with normal vasculature (Fig. 3Q). Also, the percentage of seedlings displaying fused/single cotyledon(s) is strongly decreased with respect to that observed in *hat3-3 athb4-1* (supplementary material Fig. S10 and Table S9). It is worth noting that ATHB2:GUS expression is severely impaired in hypocotyl and root of *hat3-3 athb4-1* seedlings displaying lancet and flamingo cotyledons (Fig. 3S,T), suggesting that simultaneous lack of HAT3 and ATHB4 might affect vascular development in these organs also.

The finding that ATHB2:GUS is expressed at higher levels in apical embryo domain and in SAM of *hat3-3 athb4-1* suggests that *ATHB2* might be negatively regulated by HAT3 and/or ATHB4 in these domains in wt. Several pieces of evidence support the hypothesis that HAT3 and/or ATHB4 may directly repress *ATHB2*. All HD-Zip IIγ and HD-Zip IIδ proteins contain an LxLxL type of EAR repression motif (Ciarbelli et al., 2008; Kagale et al., 2010), and there is evidence that at least some of them function as negative regulators of gene expression (Steindler et al., 1999; Ohgishi et al., 2001; Sawa et al., 2002). The upstream regions of the HD-Zip II genes, including that of *ATHB2*, are significantly enriched for HD-Zip-binding sequences (Ciarbelli et al., 2008) (Fig. 4A), and it has

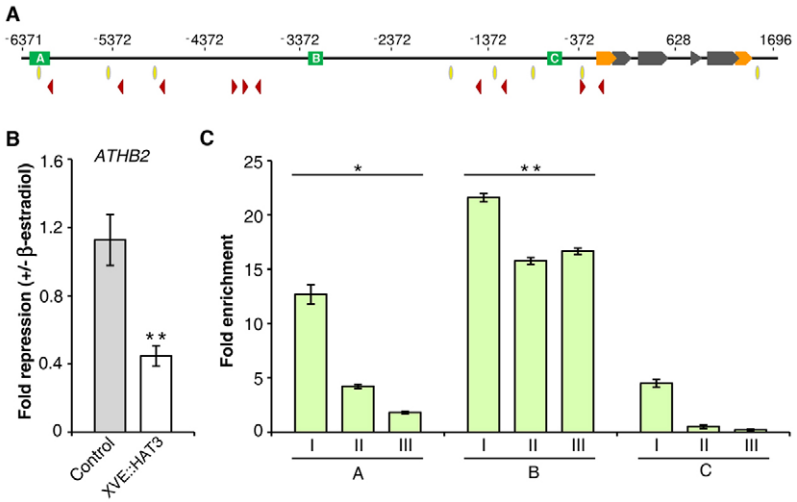

Fig. 4. *ATHB2* is a direct target of HAT3. (**A**) Schematic representation of *ATHB2*. Green boxes, DNA fragments assayed by ChIP; orange arrows, 5′UTR and 3′UTR; gray arrows, exons; yellow ovals, putative HD-Zip II-and HD-Zip III-binding sites (NNAATSATTNN); red triangles, putative HD-Zip III-binding sites (NNAATSATGNN; G.M., unpublished). (**B**) Relative expression of *ATHB2* in XVE::HAT3 seedlings after 4 hours in 50 μM β-estradiol. Control, Col-0 transformed with pER8. (**C**) Chromatin from HAT3::HAT3:GFP seedlings was immunoprecipitated with anti-GFP antibody. The fold enrichment of DNA fragments A, B and C in relation to the total chromatin input is shown for three independent experiments. Error bars represent s.d.; n=3; *P<0.05, **P<0.01, Student's t-test.

been shown that inducible chimeric proteins consisting of the DNA-binding domain of HD-Zip II proteins and the transactivation domain of VP16 (HD-Zip2-V-G; H2-V-G) directly induce the expression of all HD-Zip IIγ and HD-Zip IIδ genes *in vivo*, implying an intricate negative-feedback network within this gene family (Ciarbelli et al., 2008). Consistent with the above-mentioned hypothesis, mRNA levels of *ATHB2* were reduced after 4 hours of β-estradiol-induced HAT3 expression (Fig. 4B; supplementary material Fig. S5). To investigate whether HAT3 regulates *ATHB2* expression by physically interacting with its promoter, we performed ChIP using seedlings expressing HAT3:GFP driven by the *HAT3* promoter. Two fragments of the *ATHB2* promoter were over-represented in the immunoprecipitated chromatin, indicating direct binding to HAT3:GFP (Fig. 4C). This, together with the rapid repression of *ATHB2* expression upon HAT3 induction indicates that *ATHB2* is a direct target of HAT3.

HAT3, ATHB4 and ATHB2 act redundantly in regulating SAM activity

HAT3 and *ATHB4* are expressed in the SAM of mature embryos (see Fig. 1), suggesting that both genes also act in the early stages of shoot development. Therefore, SAM activity of *hat3-3 athb4-1* was analyzed. Almost all double mutants with two cotyledons display active SAM as deduced by the presence of leaf primordia (566/568). Consistent with this, no significant difference in the expression of *WUSCHEL* (*WUS*) and *CLAVATA3* (*CLV3*), which mark the stem cells in the SAM (Fletcher et al., 1999; Schoof et al., 2000; Gross-Hardt et al., 2002), was observed in *hat3-3 athb4-1* mutants with two cotyledons relative to wt (Fig. 5A,B,G,H). By contrast, *hat3-3 athb4-1* seedlings with fused/single cotyledon(s) could be split into two groups, one with active SAM and the other one with inactive SAM, characterized by the absence of any cell dome in the site of presumptive SAM (supplementary material Fig. S11). The former group expresses WUS::GUS and CLV3::GUS whereas the latter one does not (Fig. 5C,D,I,J).

Together, these data indicate that a significant number of *hat3-3 athb4-1* seedlings lack an active SAM, as deduced by the absence of leaf primordia (36/639, P<0.0001) or expression of WUS::GUS (9/222, P=0.0039) and CLV3::GUS (12/250, P=0.0043). The SAM phenotype was restored by HAT3::HAT3:GFP (363/364 seedlings displayed active SAM). However, the majority of *hat3-3 athb4-1* mutants do form leaf primordia. Several pieces of evidence indicate that auxin is required for lateral organ formation and that PIN1 has a key role in this process (Reinhardt et al., 2000; Reinhardt et al., 2003; Benková et al., 2003). To investigate whether there is any link between the function of HAT3 and ATHB4 and the distribution of auxin in SAM, the effects of NPA, an inhibitor of polar auxin transport, on leaf organ formation in *hat3-3 athb4-1* was analyzed. After NPA application, the fusion of first leaves was infrequently observed in wt (Fig. 5E,F). By contrast, in *hat3-3 athb4-1* first leaf fusion was greatly enhanced by NPA (Fig. 5K,L). A similar phenotype was observed in *hat3-3 athb4-3* and *hat3-2 athb4-1* (69/150 and 46/98, respectively). By contrast, in the presence of NPA the number of *hat3-3 athb4-1* HAT3::HAT3:GFP seedlings displaying fused leaves was significantly lower (30/305).

We investigated next whether the lack of ATHB2 enhances the SAM phenotype of *hat3-3 athb4-1*. Most of the *hat3-3 athb4-1 athb2-1* and *hat3-3 athb4-1 athb2-3* seedlings with two cotyledons or single cotyledon lack an active SAM (363/388 and 258/283, respectively). Among the triple mutants with two cotyledons are also present few seedlings displaying a pin-like structure in the site of presumptive SAM (10/226 and 9/158, respectively; Fig. 5M-R). The SAM phenotype of both triple mutants is dramatically more severe than that observed in *hat3-3 athb4-1* (P<0.0001). By contrast, the SAM phenotype of *hat3-3 athb4-1* is significantly attenuated by expression of ATHB2::ATHB2:GUS (4/276; P=0.0041). No significant difference was observed in SAM activity between *hat3-3 athb4-1* and *hat3-3 athb4-1 athb2-2* (36/639 and 19/331 seedlings displayed inactive SAM, respectively).

HAT3, ATHB4 and ATHB2 act redundantly in specifying adaxial identity of lateral organs

All the defects seen in *hat3 athb4* and *hat3 athb4 athb2* seedlings are reminiscent of the phenotypes observed in multiple mutants in HD-Zip III genes, master regulators of apical fate (Emery et al., 2003; Prigge et al., 2005; Smith and Long, 2010). Furthermore, both *HAT3* and *ATHB4* exhibit overlapping expression patterns with *PHB*, *PHV* and *REV* in the adaxial domain of cotyledons, in the vasculature and in the SAM (see Fig. 1) (Emery et al., 2003), suggesting that HD-Zip II and HD-Zip III genes might functionally interact. PHB, PHV and REV also function in specifying adaxial identity of lateral organs (McConnell and Barton, 1998; McConnell et al., 2001; Emery et al., 2003), and recent work provided some evidence for a role of HAT3 and ATHB4 in leaf polarity (Bou-Torrent et al., 2012). To investigate HD-Zip II function in adaxial

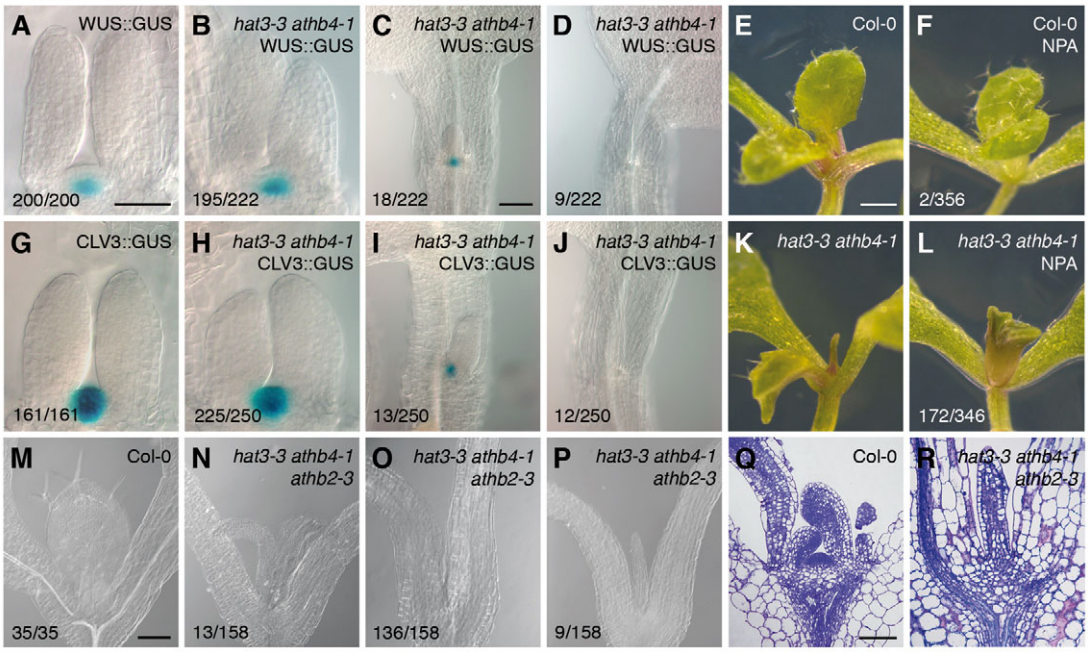

Fig. 5. SAM defects in *hat3 athb4* and *hat3 athb4 athb2* mutants. (**A-D**,**G-J**) GUS localization in WUS::GUS (A), *hat3-3 athb4-1* WUS::GUS (B-D), CLV3::GUS (G) and *hat3-3 athb4-1* CLV3::GUS (H-J) seedlings with two cotyledons and active SAM (B,H), fused/single cotyledon(s) and active (C,I) or inactive (D,J) SAM. (**E**,**F**,**K**,**L**) Col-0 (E,F) and *hat3-3 athb4-1* (K,L) seedlings grown in the presence of DMSO (E,K) or 10 μM NPA (F,L). (**M-P**) Brightfield images of Col-0 (M) and *hat3-3 athb4-1 athb2-3* (N-P) seedlings with two radialized cotyledons (158/283) and active SAM (N), inactive SAM (O) or a pin-like structure (P). (**Q**,**R**) Sections of Col-0 (Q) and *hat3-3 athb4-1 athb2-3* (R) seedlings. Scale bars: A,B,G,H, 5 μm; C,D,I,J, 10 μm; E,F,K,L, 0.5 mm; M-P, 20 μm; Q,R, 100 μm.

identity specification, we examined the polarity defects associated with *hat3* and *athb4* mutations.

A fraction of *hat3-3 athb4-1* seedlings produces two radialized cotyledons, a phenotype similar to that seen in less severely affected *phb-6 phv-5 rev-9* plants (Emery et al., 2003). As observed in these mutants, the vasculature in the radialized cotyledons of *hat3-3 athb4-1* is also radialized, with phloem surrounding the xylem (supplementary material Fig. S12). Cotyledon polarity defects were also observed in *hat3-1 athb4-1* seedlings (Bou-Torrent et al., 2012).

Simultaneous lack of HAT3 and ATHB4 also affects leaf polarity (Fig. 6A,E). Lower order leaves of *hat3-3 athb4-1* show varying degrees of expansion, from expanded to completely radialized organs, whereas higher order leaves all display a severe phenotype. The pattern of vascular development is profoundly altered in *hat3-3 athb4-1* trumpet-shaped leaves whereas *hat3-3 athb4-1* radialized leaves have no recognizable vasculature (supplementary material Fig. S13A,B). Leaf polarity defects were also observed in *hat3-1 athb4-1* (Bou-Torrent et al., 2012). Furthermore, the *hat3-3 athb4-1* leaf phenotype was completely rescued by introducing the wt *HAT3* gene in the double mutant (supplementary material Fig. S6Ce-h).

Early in development, leaf primordia establish dorsoventral polarity, which is of primary importance for proper lamina growth. Anatomical differences along the abaxial-adaxial axis of leaf primordia are evident in wt (Fig. 6B) (Eshed et al., 2004). By contrast, leaf primordia of *hat3-3 athb4-1* were nearly radial with large vacuolated cells on both adaxial and abaxial sides (Fig. 6F). Consistent with a role of the HD-Zip IIδ proteins in specifying organ polarity, HAT3::GUS and ATHB4::GUS expression in leaf primordia is restricted to the adaxial domain (Fig. 6C,D; supplementary material Fig. S5). To characterize further the polar nature of *hat3-3 athb4-1* leaf primordia, abaxial-specific gene expression in the mutant was assessed. To this end, we analyzed *YAB3* expression in *hat3-3 athb4-1* using the *yab3-2* gene trap line, which faithfully reproduces *YABBY3* (*YAB3*) expression in leaves (YAB3::GUS) (Kumaran et al., 2002). GUS activity was detected uniformly throughout first leaf primordia in a significant number of *hat3-3 athb4-1* YAB3::GUS/+ descendants whereas it was restricted to the abaxial domain of the young lateral organs of YAB3::GUS plants (Fig. 6G,H; P=0.0001). The expressivity of the phenotype in the first leaves of *hat3-3 athb4-1* plants is variable, and it seems likely that the observed uniform expression of YAB3::GUS is associated with radialized primordia. Consistent with this, YAB3::GUS was expressed both in the adaxial and abaxial regions of the third and fourth leaf primordia of almost all the *hat3-3 athb4-1* YAB3::GUS/+ descendants with detectable β-glucuronidase activity (56/61) whereas it was restricted to the abaxial domain in YAB3::GUS plants (58/58). Thus, simultaneous lack of both HAT3 and ATHB4 is associated with loss of adaxial identity.

We then assessed whether ATHB2:GUS expression attenuates the leaf phenotype of *hat3-3 athb4-1*. Leaf development defects in *hat3-3 athb4-1* ATHB2::ATHB2:GUS were significantly less severe than those of *hat3-3 athb4-1* (Fig. 6I,J; supplementary material Fig. S13C). In ATHB2::ATHB2:GUS leaf primordia, GUS activity was detected exclusively in provascular cells. By contrast, a significant number of *hat3-3 athb4-1* plants also express ATHB2:GUS in the adaxial domain of leaf primordia (Fig. 6K,L; P<0.0001). A GFP-tagged ATHB2 driven by the 35S promoter is uniformly expressed in leaf primordia (Fig. 6M; supplementary material Fig. S5), indicating that ATHB2 expression is largely regulated at the transcriptional and/or post-transcriptional level. We then investigated whether ectopic expression of ATHB2 would result in upward leaf curling, which is usually observed when HD-Zip III

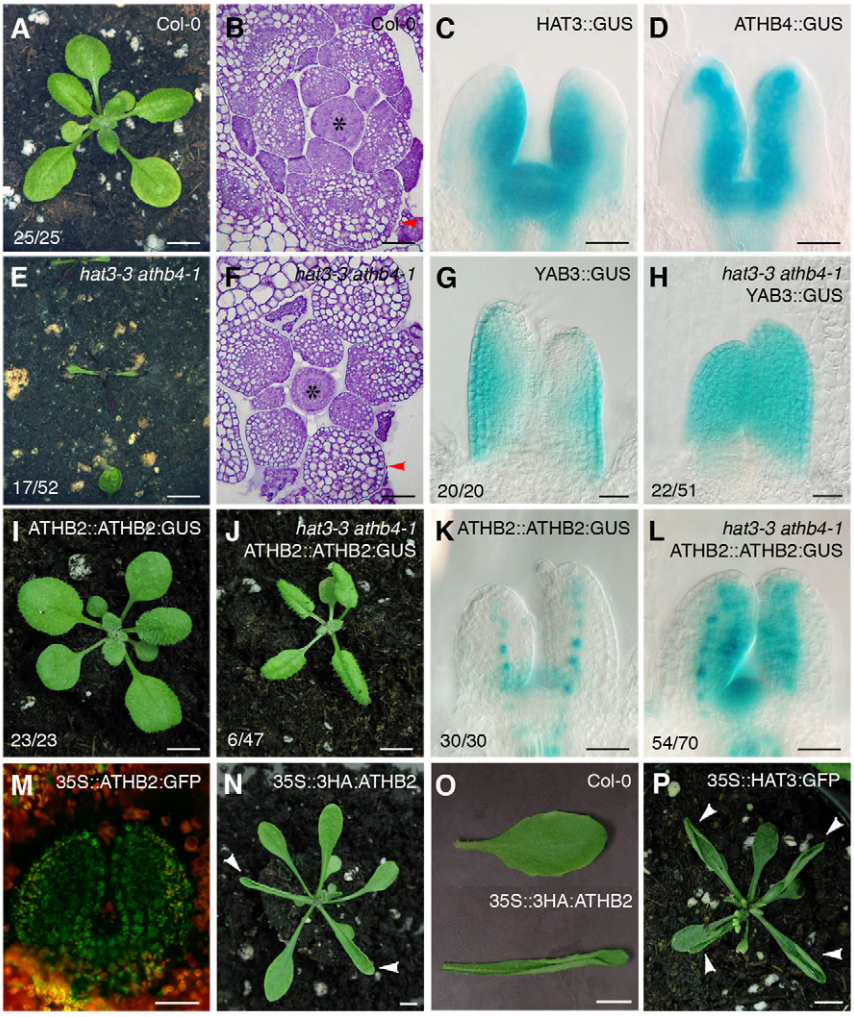

Fig. 6. HD-Zip II proteins control leaf polarity. (**A**,**E**) Col-0 (A) and *hat3-3 athb4-1* (E) plants. (**B**,**F**) Transverse sections at the level of the SAM (asterisks) of Col-0 (B) and *hat3-3 athb4-1* (F) plants. (**C**,**D**,**G**,**H**) GUS localization in HAT3::GUS (C), ATHB4::GUS (D), YAB3::GUS (G) and *hat3-3 athb4-1* YAB3::GUS (H) seedlings. (**I**,**J**) ATHB2::ATHB2:GUS (I) and *hat3-3 athb4-1* ATHB2::ATHB2:GUS (J) plants. (**K**,**L**) GUS localization in ATHB2::ATHB2:GUS (K) and *hat3-3 athb4-1* ATHB2::ATHB2:GUS (L) seedlings. (**M**) GFP fluorescence in 35S::ATHB2:GFP leaf primordia. (**N**,**P**) 35S::3HA:ATHB2 (N) and 35S::HAT3:GFP (P) plants. (**O**) Sixth leaf from Col-0 (upper) and 35S::3HA:ATHB2 (lower). Red arrowheads, seventh leaf primordia; white arrowheads, leaves displaying upward curling. Scale bars: C,D,G,H,K-M, 30 μm; B,F, 50 μm; A,E,I,J,N-P, 5 mm.

genes are resistant to regulation by miRNAs and thus expressed in both adaxial and abaxial regions of lateral organs (Juarez et al., 2004; Mallory et al., 2004; Ochando et al., 2006; Ochando et al., 2008). Remarkably, 35S::3HA:ATHB2 leaves are severely curled upwards (Fig. 6N,O; supplementary material Fig. S5). The same phenotype was also observed in 35S::HAT3:GFP and in 35S::ATHB4:GFP (Fig. 6P; supplementary material Fig. S5; data not shown), and in dexamethasone (DEX)-treated 35S::FLAG-GR-HAT3 plants (Bou-Torrent et al., 2012).

Genetic interaction between HD-Zip II and HD-Zip III genes

To gain further insights on the relationships between HD-Zip IIδ genes and *PHB*, *PHV* and *REV*, we examined their genetic interactions.

phv and *phb* resemble wt (Emery et al., 2003; Prigge et al., 2005), and lack of either PHV or PHB in *hat3-3* and *athb4-1* does not result in any obvious phenotype (n>175). We then isolated and characterized *hat3-3/+ athb4-1 phv-11* and *hat3-3 athb4-1/+ phb-13* (supplementary material Tables S10-S12). To evaluate whether lack of PHV or PHB enhances the developmental defects of *hat3-3 athb4-1*, the SAM phenotype of *hat3-3 athb4-1 phv-11* and *hat3-3 athb4-1 phb-13* seedlings with two cotyledons was analyzed. A significant number of both triple mutants lack an active SAM (supplementary material Fig. S14; Fig. 7A,B; P≤0.0001). Loss of PHV but not PHB also enhances *hat3-3 athb4-1* defects in bilateral symmetry (supplementary material Fig. S14; P<0.0212). Furthermore, a significant number of embryos isolated from *hat3-3 athb4-1/+ phb-13* plants display embryo lethality (Fig. 7C,D), probably because of failure to establish normal patterning (Fig. 7E-H). Among the progeny of *hat3-3 athb4-1/+ phb-13*, two-cell pro-embryos in which the apical cell divided horizontally rather than vertically were observed (P<0.0001), suggesting that HD-Zip II and HD-Zip III proteins may influence cell division planes in early embryo development.

rev mutants fail to produce axillary meristems and functional floral meristems, and exhibit alterations in the position of interfascicular fibers in the stem (Talbert et al., 1995; Zhong and Ye, 1999; Ratcliffe et al., 2000; Otsuga et al., 2001). *hat3-3 rev-5* (718/723) and *athb4-1 rev-5* (60/60) display the *rev* phenotype at late stages of development, and are largely indistinguishable from wt at the seedling stage. We then isolated and characterized *hat3-3 athb4-1/+ rev-5* (supplementary material Tables S10, S13). Almost all *hat3-3 athb4-1 rev-5* seedlings with two cotyledons as well as those with single cotyledon (Fig. 7I-L; supplementary material Fig. S14) lack an active SAM (*hat3-3 athb4-1*, 1/224; *hat3-3 athb4-1 rev-5*, 24/30; P<0.0001). Loss of REV also significantly enhances *hat3-3 athb4-1* defects in bilateral symmetry (supplementary material Fig. S14; P<0.0001).

ATHB2 is a direct target of REV

To examine whether HD-Zip II and HD-Zip III genes also interact at the molecular level, *ATHB2* was selected for further

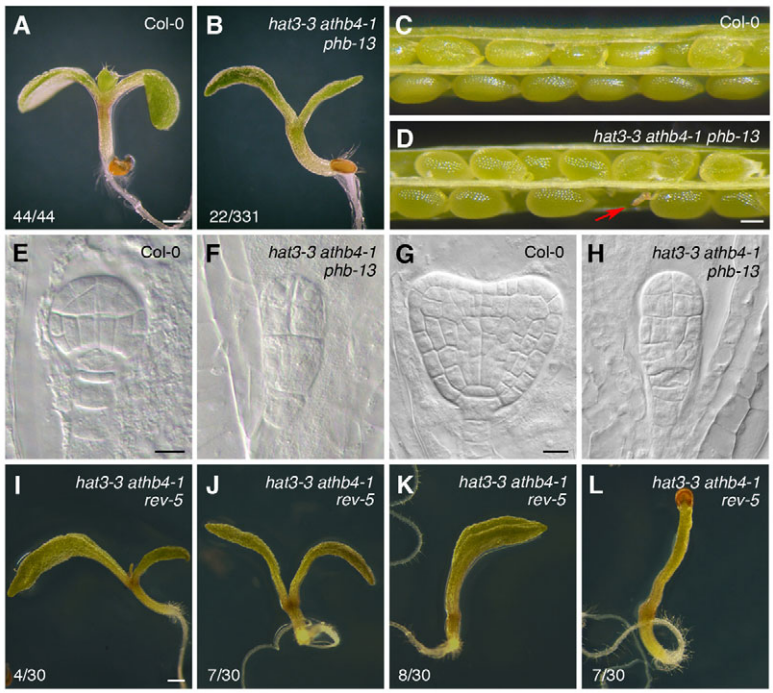

Fig. 7. Loss of PHB or REV enhances developmental defects in *hat3 athb4* mutants. (**A**,**B**) Col-0 (A) and *hat3-3 athb4-1 phb-13* (B) seedlings. (**C**,**D**) Siliques of Col-0 (C) and *hat3-3 athb4-1/+ phb-13* (D) plants. Normal seeds and dark, shriveled seeds (red arrow) occur in siliques of *hat3-3 athb4-1/+ phb-13* (Col-0: 30/2029; *hat3-3 athb4-1/+ phb-13*: 121/2404; $P<0.0001$). (**E-H**) Siliques with embryos at the globular (E,F) and heart (G,H) stages were collected from Col-0 (E,G) and *hat3-3 athb4-1/+ phb-13* (F,H). The frequency of embryos with severe patterning defects was significantly higher in siliques from mutant (F,H) than Col-0 (E,G) (41/948 and 4/839, respectively; $P<0.0001$). (**I-L**) *hat3-3 athb4-1 rev-5* seedlings. Scale bars: A,B,I,J-L, 0.5 mm; C,D, 0.2 mm; E-H, 10 μm.

investigations. Induction of HD-Zip-2-V-G does not result in any significant change in the expression of the HD-Zip III genes (supplementary material Fig. S15), therefore it is unlikely that the ATHB2 DNA-binding domain interacts physically with HD-Zip III genes. HD-Zip II- and HD-Zip III-binding sites share the same core sequence (AAT[G/C]ATT) (Sessa et al., 1993; Sessa et al., 1998), thus suggesting that *ATHB2* might physically interact not only with HAT3 but also with one or more member of the HD-Zip III protein family. Consistent with this hypothesis, ChIP-Seq using plants expressing a FLAG-tagged ligand-binding domain of the glucocorticoid receptor, fused to a microRNA-resistant version of REV under control of the 35S-promoter (35S::FLAG-GR-REVd) identified loci with the motif AT[G/C]AT, including the promoter regions of several HD-Zip II genes (Brandt et al., 2012). To investigate further whether REV physically interacts with *ATHB2*, we performed ChIP using *rev-5* seedlings expressing REV:GFP driven by the *REV* promoter, which complements the mutant phenotype (Lee et al., 2006) (G.M., unpublished). Fragment C of the *ATHB2* promoter was over-represented in the immunoprecipitated chromatin, demonstrating direct binding to REV:GFP (Fig. 8A; see Fig. 4A). By contrast, no reproducibility of the ChIP results was observed with fragment A of the *ATHB2* promoter (Fig. 8A), previously reported to be over-represented in the immunoprecipitated chromatin of DEX-treated 35S::FLAG-GR-REVd (Brandt et al., 2012).

The role of HD-Zip III proteins in the regulation of *ATHB2* was examined further by analyzing *ATHB2* mRNA in single and double HD-Zip III mutants displaying a wt phenotype at the seedling stage and in plants expressing an inducible miR 165/166-resistant variant of *ATHB8* (ATHB8d; supplementary material Fig. S5). In the presence of β-estradiol, XVE::ATHB8d plants display upward leaf curling (data not shown), as observed with miR 165/166-resistant variants of other HD-Zip III genes (Juarez et al., 2004; Mallory et al., 2004; Ochando et al., 2006; Ochando et al., 2008). *ATHB2* mRNA levels were reduced in *rev-5* and *phv-11 phb-13* and increased after 4 hours of β-estradiol-induced ATHB8d expression (Fig. 8B,C). Higher *ATHB2* mRNA levels have also been observed in DEX-treated 35S::FLAG-GR-REVd plants (Brandt et al., 2012). Together, the data indicate that *ATHB2* is a direct target of REV and that HD-Zip III proteins other than REV are also involved in *ATHB2* regulation.

DISCUSSION

In this study, we demonstrate a crucial role for HD-Zip IIδ proteins in embryo development. Simultaneous lack of HAT3 and ATHB4 results in striking cotyledon phenotypes and defects in bilateral symmetry. Auxin maxima and distribution are also altered in *hat3 athb4*, indicating a link between auxin-mediated embryo patterning and HD-Zip IIδ function. Auxin maxima formation at the sites of incipient cotyledons largely depends on changes in auxin flow occurring at the transition stage. PIN1 is expressed throughout the apical embryo during the globular stage, but later, at the transition stage, resolves into domains of higher expression that mark the sites of cotyledon initiation (Benková et al., 2003). Mutations that cause altered PIN1 expression or polarity during the transition stage affect bilateral symmetry (Izhaki and Bowman, 2007; Michniewicz et al., 2007; Ploense et al., 2009). The low number of embryos with single cotyledon in the progeny of *hat3-3/+ athb4-1* prevented us from analyzing PIN1:GFP pattern at the early stages of development. However, it seems likely that the single DR5::GFP maximum observed in mature *hat3-3 athb4-1* embryos with a single expanded cotyledon reflects defects in PIN1 expression pattern at the transition stage. The interplay between auxin and its efflux transporter PIN1 is also important in organ separation at the SAM. *pin1* mutants display leaf fusion defects (Reinhardt et al., 2003), and failure in leaf separation is evident in plants lacking MP in the presence of NPA (Donner et al., 2009). Furthermore, mutations in *NO VEIN* (*NOV*), which encodes a nuclear factor required for cotyledon outgrowth and separation, leaf vascular development, and stem cell maintenance in RAM, also enhance leaf organ fusion in the presence of NPA (Tsugeki et al., 2009). *NOV* genetically interacts with *GNOM*, a gene encoding an ARF GDP/GTP exchange factor involved in proper subcellular localization of PIN proteins (Steinmann et al., 1999; Geldner et al., 2003; Kleine-Vehn et al., 2008), and is required for provascular PIN1

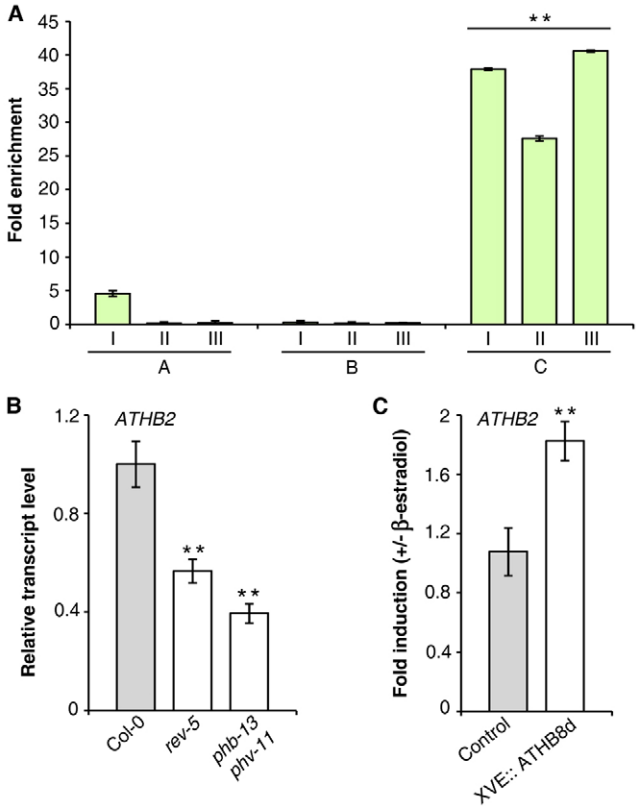

Fig. 8. ATHB2 expression is directly regulated by REV. (**A**) Chromatin from *rev-5* REV::REV:GFP seedlings was immunoprecipitated with anti-GFP antibody. The fold enrichment of DNA fragments A, B and C in relation to the total chromatin input is shown for three independent experiments. (**B**,**C**) Relative expression of *ATHB2* in *rev-5*, *phv-11 phb-13* and XVE::ATHB8d seedlings after 4 hours in 50 µM β-estradiol. Control, Col-0 transformed with pER10. Error bars represent s.d.; n=3; $^{**}P$<0.01, Student's t-test.

expression and region-specific expression of PIN7 in leaf primordia (Tsugeki et al., 2009). Significantly, we find that mutations in *HAT3* and *ATHB4* strongly enhance leaf organ fusion in the presence of NPA, thus demonstrating augmented sensitivity of *hat3 athb4* to auxin transport inhibition.

HD-Zip IIγ and HD-Zip IIδ proteins contain an LxLxL type of EAR repression motif (Ciarbelli et al., 2008; Kagale et al., 2010) and behave as negative regulators of gene expression (Ohgishi et al., 2001; Sawa et al., 2002). All HD-Zip II promoters are significantly enriched for HD-Zip-binding sequences, suggesting that members of this family negatively regulate each other (Ciarbelli et al., 2008). Here, we demonstrate that HAT3 and ATHB4 exhibit synergistic interaction with HD-Zip IIγ proteins, which involves cross-regulation within the two subfamilies. The finding that ATHB2 became induced in the *HAT3-ATHB4* expression domain in the apical part of the embryo, marking the incipient cotyledons, as well as in the SAM of *hat3 athb4*, and thus can at least partially compensate for HAT3 and ATHB4 function, indicates that HD-Zip IIγ and HD-Zip IIδ proteins are to some extent functionally interchangeable. In agreement, *athb2* loss-of-function mutations significantly enhance the *hat3 athb4* phenotype. Almost all *hat3 athb4 athb2* mutants display radialized cotyledons and, among these, more than one-third shows loss of bilateral symmetry. Furthermore, gain-of-function mutation in *ATHB2* significantly attenuates the *hat3 athb4* phenotype. The discovery that HAT3:GFP physically interacts with two *ATHB2* promoter fragments, as determined by ChIP, together with the rapid repression of *ATHB2* expression upon HAT3 induction indicate that *ATHB2* is indeed a direct target of HAT3.

A significant number of *hat3 athb4* seedlings also lack active SAM and fail to express shoot stem cell niche-specific markers. The SAM phenotype in *hat3 athb4* is strictly linked to defects in bilateral symmetry. By contrast, essentially all *hat3 athb4* seedlings with two cotyledons form leaves that display severe polarity defects (Bou-Torrent et al., 2012) (this work). The abaxial marker *YAB3* (Kumaran et al., 2002) is uniformly expressed throughout leaf primordia of *hat3 athb4*, thus demonstrating that simultaneous lack of *HAT3* and *ATHB4* is associated with loss of adaxial identity. The ectopic expression of HAT3, ATHB4 or ATHB2 results in upward leaf curling, a phenotype similar to that seen when HD-Zip III genes are expressed in both adaxial and abaxial regions of lateral organs (Juarez et al., 2004; Mallory et al., 2004; Ochando et al., 2006; Ochando et al., 2008). ATHB2:GUS was induced in the HAT3-ATHB4 domain on the adaxial side of leaf primordia of *hat3 athb4*, thus leading to an attenuation of the phenotype. By contrast, loss-of-function mutations in *ATHB2* significantly enhance the SAM phenotype of *hat3 athb4*. Indeed, most of the triple mutants lack an active SAM, displaying a phenotype similar to that of multiple HD-Zip III loss-of-function mutants. A few of the *hat3 athb4 athb2* seedlings with two cotyledons show a pin-like structure that lacks a vascular strand in the site of presumptive SAM, which is reminiscent of the phenotype of loss of PINHEAD (PNH; also known as ZWILLE and ARGONAUTE 10) (Lynn et al., 1999; Moussian et al., 1998). The primary cause of the severe SAM defects in *pnh* seems to be the accumulation of miR 165 and miR 166 and the consequent downregulation of the HD-Zip III mRNAs in the SAM (Liu et al., 2009).

All double and triple HD-Zip II mutant phenotypes described here are indeed reminiscent of those seen in *phb rev* and *phb phv rev* (Emery et al., 2003; Prigge et al., 2005), suggesting that HD-Zip II and HD-Zip III proteins may cooperate in establishing bilateral symmetry in the embryo as well as in controlling SAM activity. Consistent with the overlapping expression pattern of HD-Zip II and HD-Zip III gene family members, loss-of-function mutations in *PHV*, *PHB* or *REV* enhance the SAM phenotype of *hat3 athb4*. Loss of PHV and, to an even greater extent, of REV also augments the defects in bilateral symmetry of *hat3 athb4*. Furthermore, a fraction of *hat3 athb4 phb* mutants display abnormal cell divisions at the early stages of embryo development and fail to complete embryogenesis. The functional interaction between HD-Zip II and HD-Zip III genes is further corroborated by the discovery that *ATHB2* interacts not only with HAT3 but also with REV. This, together with the finding that *ATHB2* expression is reduced in *rev* and *phv phb* but is rapidly induced in plants expressing an inducible miR 165/166-resistant variant of *ATHB8*, establishes *ATHB2* as a component of developmental pathway(s) regulated by REV and, probably, by other members of the HD-Zip III family.

The finding that ATHB2 is positively regulated by REV and negatively regulated by HAT3 highlights the potential complexity of regulatory interactions among HD-Zip II and HD-Zip III proteins. There is some recent evidence that closely related sub-family members might share regulation of target genes through redundant promoter occupancy, in a way that varies quantitatively from gene to gene (Zhang et al., 2013). In this scenario, the expression pattern of each HD-Zip II gene in white light would depend on its responsiveness to the different HD-Zip III family members, levels of which are tightly regulated during development. The negative-feedback network within the HD-Zip II family adds an additional level of complexity. The relative level of each HD-Zip II protein is

likely to influence significantly this feedback. For example, ATHB2, which is strongly induced by changes in light quality, has a central role in negatively regulating HD-Zip IIγ and HD-ZipIIδ genes at late stages of shade avoidance (G.S., unpublished).

In conclusion, we uncover a crucial role for *HAT3*, *ATHB4* and *ATHB2* in embryo development and SAM activity, and provide evidence for genetic and molecular interaction between HD-Zip II and HD-Zip III genes, which are primary determinants of apical shoot development. HD-Zip IIγ and HD-Zip IIδ genes are mostly known for their role in shade avoidance (Ruberti et al., 2012), and evidence exists that at least *ATHB2* is a direct target of PHYTOCHROME INTERACTING FACTOR4 (PIF4) and PIF5 (Hornitschek et al., 2012). Low red (R)/far red (FR) light rapidly induces ATHB2:GUS expression in all cell layers of the elongating portion of the hypocotyl and cotyledon petioles (V.R., unpublished), thus suggesting that ATHB2 acts, at least in part, in these organs to control shade avoidance. *HAT3*, *ATHB4*, *ATHB2* and *HAT1* (also known as *JAIBA*) (Zúñiga-Mayo et al., 2012) were also recently identified as genes positively regulated by SPATULA, a basic helix-loop-helix (bHLH) protein related to PIFs but lacking the active phytochrome-binding domain involved in their negative regulation by the phytochrome in high R/FR, and were proposed to be involved in carpel margin development (Reymond et al., 2012). Given the dual role of HD-Zip II proteins in development and in shade avoidance, it will be interesting to identify target genes and regulatory modules in high and low R/FR in specific cell types and to understand how HD-Zip II factors impinge on embryo patterning as well as on plant response to changes in the light environment.

Acknowledgements
We thank Philip Benfey, Luca Comai, Mark Curtis, Jiří Friml, Sergei Kushnir, Thomas Laux, Nottingham *Arabidopsis* Stock Centre and Cold Spring Harbor Laboratory for providing seeds and constructs. We are grateful to Angela Ciarbelli and Carmen Melatti for preliminary analysis of HD-Zip II and HD-Zip II/HD-Zip III alleles; Alberto Fruscalzo for generating the HAT3::HAT3:GFP construct; and Daniela Bongiorno for technical assistance.

Funding
This work was supported, in part, by the Ministry of Education, University and Research: Fondo per gli Interventi alla Ricerca di Base – European Research Area Networks in Plant Genomics (FIRB-ERA-PG) program; the Ministry of Agricultural, Food and Forestry Policies: AGRONANOTECH and NUTRIGEA programs; the Ministry of Economy and Finance: FaReBio di Qualità program.

Competing interests statement
The authors declare no competing financial interests.

Supplementary material
Supplementary material available online at
http://dev.biologists.org/lookup/suppl/doi:10.1242/dev.092833/-/DC1

References

Aida, M., Beis, D., Heidstra, R., Willemsen, V., Blilou, I., Galinha, C., Nussaume, L., Noh, Y. S., Amasino, R. and Scheres, B. (2004). The PLETHORA genes mediate patterning of the Arabidopsis root stem cell niche. *Cell* **119**, 109-120.
Babiychuk, E., Fuangthong, M., Van Montagu, M., Inzé, D. and Kushnir, S. (1997). Efficient gene tagging in Arabidopsis thaliana using a gene trap approach. *Proc. Natl. Acad. Sci. USA* **94**, 12722-12727.
Benková, E., Michniewicz, M., Sauer, M., Teichmann, T., Seifertová, D., Jürgens, G. and Friml, J. (2003). Local, efflux-dependent auxin gradients as a common module for plant organ formation. *Cell* **115**, 591-602.
Berleth, T. and Jürgens, G. (1993). The role of the monopteros gene in organising the basal body region of the Arabidopsis embryo. *Development* **118**, 575-587.
Blilou, I., Xu, J., Wildwater, M., Willemsen, V., Paponov, I., Friml, J., Heidstra, R., Aida, M., Palme, K. and Scheres, B. (2005). The PIN auxin efflux facilitator network controls growth and patterning in Arabidopsis roots. *Nature* **433**, 39-44.
Bou-Torrent, J., Salla-Martret, M., Brandt, R., Musielak, T., Palauqui, J. C., Martinez-Garcia, J. F. and Wenkel, S. (2012). ATHB4 and HAT3, two class II HD-ZIP transcription factors, control leaf development in Arabidopsis. *Plant Signal. Behav.* **7**, 1382-1387.
Brandt, R., Salla-Martret, M., Bou-Torrent, J., Musielak, T., Stahl, M., Lanz, C., Ott, F., Schmid, M., Greb, T., Schwarz, M. et al. (2012). Genome-wide binding-site analysis of REVOLUTA reveals a link between leaf patterning and light-mediated growth responses. *Plant J.* **72**, 31-42.
Carabelli, M., Possenti, M., Sessa, G., Ciolfi, A., Sassi, M., Morelli, G. and Ruberti, I. (2007). Canopy shade causes a rapid and transient arrest in leaf development through auxin-induced cytokinin oxidase activity. *Genes Dev.* **21**, 1863-1868.
Chandler, J. W. (2008). Cotyledon organogenesis. *J. Exp. Bot.* **59**, 2917-2931.
Chandler, J. W., Cole, M., Flier, A., Grewe, B. and Werr, W. (2007). The AP2 transcription factors DORNROSCHEN and DORNROSCHEN-LIKE redundantly control Arabidopsis embryo patterning via interaction with PHAVOLUTA. *Development* **134**, 1653-1662.
Ciarbelli, A. R., Ciolfi, A., Salvucci, S., Ruzza, V., Possenti, M., Carabelli, M., Fruscalzo, A., Sessa, G., Morelli, G. and Ruberti, I. (2008). The Arabidopsis homeodomain-leucine zipper II gene family: diversity and redundancy. *Plant Mol. Biol.* **68**, 465-478.
Cole, M., Chandler, J., Weijers, D., Jacobs, B., Comelli, P. and Werr, W. (2009). DORNROSCHEN is a direct target of the auxin response factor MONOPTEROS in the Arabidopsis embryo. *Development* **136**, 1643-1651.
De Smet, I., Lau, S., Mayer, U. and Jürgens, G. (2010). Embryogenesis – the humble beginnings of plant life. *Plant J.* **61**, 959-970.
Donner, T. J., Sherr, I. and Scarpella, E. (2009). Regulation of preprocambial cell state acquisition by auxin signaling in Arabidopsis leaves. *Development* **136**, 3235-3246.
Emery, J. F., Floyd, S. K., Alvarez, J., Eshed, Y., Hawker, N. P., Izhaki, A., Baum, S. F. and Bowman, J. L. (2003). Radial patterning of Arabidopsis shoots by class III HD-ZIP and KANADI genes. *Curr. Biol.* **13**, 1768-1774.
Eshed, Y., Izhaki, A., Baum, S. F., Floyd, S. K. and Bowman, J. L. (2004). Asymmetric leaf development and blade expansion in Arabidopsis are mediated by KANADI and YABBY activities. *Development* **131**, 2997-3006.
Fletcher, J. C., Brand, U., Running, M. P., Simon, R. and Meyerowitz, E. M. (1999). Signaling of cell fate decisions by CLAVATA3 in Arabidopsis shoot meristems. *Science* **283**, 1911-1914.
Floyd, S. K. and Bowman, J. L. (2004). Gene regulation: ancient microRNA target sequences in plants. *Nature* **428**, 485-486.
Friml, J., Vieten, A., Sauer, M., Weijers, D., Schwarz, H., Hamann, T., Offringa, R. and Jürgens, G. (2003). Efflux-dependent auxin gradients establish the apical-basal axis of Arabidopsis. *Nature* **426**, 147-153.
Galinha, C., Hofhuis, H., Luijten, M., Willemsen, V., Blilou, I., Heidstra, R. and Scheres, B. (2007). PLETHORA proteins as dose-dependent master regulators of Arabidopsis root development. *Nature* **449**, 1053-1057.
Geldner, N., Anders, N., Wolters, H., Keicher, J., Kornberger, W., Muller, P., Delbarre, A., Ueda, T., Nakano, A. and Jürgens, G. (2003). The Arabidopsis GNOM ARF-GEF mediates endosomal recycling, auxin transport, and auxin-dependent plant growth. *Cell* **112**, 219-230.
Gray, W. M., Kepinski, S., Rouse, D., Leyser, O. and Estelle, M. (2001). Auxin regulates SCF(TIR1)-dependent degradation of AUX/IAA proteins. *Nature* **414**, 271-276.
Grigg, S. P., Galinha, C., Kornet, N., Canales, C., Scheres, B. and Tsiantis, M. (2009). Repression of apical homeobox genes is required for embryonic root development in Arabidopsis. *Curr. Biol.* **19**, 1485-1490.
Gross-Hardt, R., Lenhard, M. and Laux, T. (2002). WUSCHEL signaling functions in interregional communication during Arabidopsis ovule development. *Genes Dev.* **16**, 1129-1138.
Guilfoyle, T. J. and Hagen, G. (2007). Auxin response factors. *Curr. Opin. Plant Biol.* **10**, 453-460.
Hamann, T., Benková, E., Bäurle, I., Kientz, M. and Jürgens, G. (2002). The Arabidopsis BODENLOS gene encodes an auxin response protein inhibiting MONOPTEROS-mediated embryo patterning. *Genes Dev.* **16**, 1610-1615.
Hejátko, J., Blilou, I., Brewer, P. B., Friml, J., Scheres, B. and Benková, E. (2006). In situ hybridization technique for mRNA detection in whole mount Arabidopsis samples. *Nat. Protoc.* **1**, 1939-1946.
Hornitschek, P., Kohnen, M. V., Lorrain, S., Rougemont, J., Ljung, K., López-Vidriero, I., Franco-Zorrilla, J. M., Solano, R., Trevisan, M., Pradervand, S. et al. (2012). Phytochrome interacting factors 4 and 5 control seedling growth in changing light conditions by directly controlling auxin signaling. *Plant J.* **71**, 699-711.
Izhaki, A. and Bowman, J. L. (2007). KANADI and class III HD-Zip gene families regulate embryo patterning and modulate auxin flow during embryogenesis in Arabidopsis. *Plant Cell* **19**, 495-508.
Juarez, M. T., Kui, J. S., Thomas, J., Heller, B. A. and Timmermans, M. C. P. (2004). microRNA-mediated repression of rolled leaf1 specifies maize leaf polarity. *Nature* **428**, 84-88.

Kagale, S., Links, M. G. and Rozwadowski, K. (2010). Genome-wide analysis of ethylene-responsive element binding factor-associated amphiphilic repression motif-containing transcriptional regulators in Arabidopsis. *Plant Physiol.* **152**, 1109-1134.
Khanna, R., Shen, Y., Toledo-Ortiz, G., Kikis, E. A., Johannesson, H., Hwang, Y. S. and Quail, P. H. (2006). Functional profiling reveals that only a small number of phytochrome-regulated early-response genes in Arabidopsis are necessary for optimal deetiolation. *Plant Cell* **18**, 2157-2171.
Kleine-Vehn, J., Dhonukshe, P., Sauer, M., Brewer, P. B., Wiśniewska, J., Paciorek, T., Benková, E. and Friml, J. (2008). ARF GEF-dependent transcytosis and polar delivery of PIN auxin carriers in Arabidopsis. *Curr. Biol.* **18**, 526-531.
Kumaran, M. K., Bowman, J. L. and Sundaresan, V. (2002). YABBY polarity genes mediate the repression of KNOX homeobox genes in Arabidopsis. *Plant Cell* **14**, 2761-2770.
Lau, S., Slane, D., Herud, O., Kong, J. and Jürgens, G. (2012). Early embryogenesis in flowering plants: setting up the basic body pattern. *Annu. Rev. Plant Biol.* **63**, 483-506.
Lee, J. Y., Colinas, J., Wang, J. Y., Mace, D., Ohler, U. and Benfey, P. N. (2006). Transcriptional and posttranscriptional regulation of transcription factor expression in Arabidopsis roots. *Proc. Natl. Acad. Sci. USA* **103**, 6055-6060.
Liu, Q., Yao, X., Pi, L., Wang, H., Cui, X. and Huang, H. (2009). The ARGONAUTE10 gene modulates shoot apical meristem maintenance and establishment of leaf polarity by repressing miR165/166 in Arabidopsis. *Plant J.* **58**, 27-40.
Long, J. A., Ohno, C., Smith, Z. R. and Meyerowitz, E. M. (2006). TOPLESS regulates apical embryonic fate in Arabidopsis. *Science* **312**, 1520-1523.
Lynn, K., Fernandez, A., Aida, M., Sedbrook, J., Tasaka, M., Masson, P. and Barton, M. K. (1999). The PINHEAD/ZWILLE gene acts pleiotropically in Arabidopsis development and has overlapping functions with the ARGONAUTE1 gene. *Development* **126**, 469-481.
Mallory, A. C., Reinhart, B. J., Jones-Rhoades, M. W., Tang, G., Zamore, P. D., Barton, M. K. and Bartel, D. P. (2004). MicroRNA control of PHABULOSA in leaf development: importance of pairing to the microRNA 5′ region. *EMBO J.* **23**, 3356-3364.
McConnell, J. R. and Barton, M. K. (1998). Leaf polarity and meristem formation in Arabidopsis. *Development* **125**, 2935-2942.
McConnell, J. R., Emery, J., Eshed, Y., Bao, N., Bowman, J. and Barton, M. K. (2001). Role of PHABULOSA and PHAVOLUTA in determining radial patterning in shoots. *Nature* **411**, 709-713.
Michniewicz, M., Zago, M. K., Abas, L., Weijers, D., Schweighofer, A., Meskiene, I., Heisler, M. G., Ohno, C., Zhang, J., Huang, F. et al. (2007). Antagonistic regulation of PIN phosphorylation by PP2A and PINOID directs auxin flux. *Cell* **130**, 1044-1056.
Möller, B. and Weijers, D. (2009). Auxin control of embryo patterning. *Cold Spring Harb. Perspect. Biol.* **1**, a001545.
Moussian, B., Schoof, H., Haecker, A., Jürgens, G. and Laux, T. (1998). Role of the ZWILLE gene in the regulation of central shoot meristem cell fate during Arabidopsis embryogenesis. *EMBO J.* **17**, 1799-1809.
Nakayama, N., Arroyo, J. M., Simorowski, J., May, B., Martienssen, R. and Irish, V. F. (2005). Gene trap lines define domains of gene regulation in Arabidopsis petals and stamens. *Plant Cell* **17**, 2486-2506.
Ochando, I., Jover-Gil, S., Ripoll, J. J., Candela, H., Vera, A., Ponce, M. R., Martínez-Laborda, A. and Micol, J. L. (2006). Mutations in the microRNA complementarity site of the INCURVATA4 gene perturb meristem function and adaxialize lateral organs in arabidopsis. *Plant Physiol.* **141**, 607-619.
Ochando, I., González-Reig, S., Ripoll, J. J., Vera, A. and Martínez-Laborda, A. (2008). Alteration of the shoot radial pattern in Arabidopsis thaliana by a gain-of-function allele of the class III HD-Zip gene INCURVATA4. *Int. J. Dev. Biol.* **52**, 953-961.
Ohgishi, M., Oka, A., Morelli, G., Ruberti, I. and Aoyama, T. (2001). Negative autoregulation of the Arabidopsis homeobox gene ATHB-2. *Plant J.* **25**, 389-398.
Otsuga, D., DeGuzman, B., Prigge, M. J., Drews, G. N. and Clark, S. E. (2001). REVOLUTA regulates meristem initiation at lateral positions. *Plant J.* **25**, 223-236.
Ploense, S. E., Wu, M. F., Nagpal, P. and Reed, J. W. (2009). A gain-of-function mutation in IAA18 alters Arabidopsis embryonic apical patterning. *Development* **136**, 1509-1517.
Prigge, M. J., Otsuga, D., Alonso, J. M., Ecker, J. R., Drews, G. N. and Clark, S. E. (2005). Class III homeodomain-leucine zipper gene family members have overlapping, antagonistic, and distinct roles in Arabidopsis development. *Plant Cell* **17**, 61-76.
Ratcliffe, O. J., Riechmann, J. L. and Zhang, J. Z. (2000). INTERFASCICULAR FIBERLESS1 is the same gene as REVOLUTA. *Plant Cell* **12**, 315-317.
Reinhardt, D., Mandel, T. and Kuhlemeier, C. (2000). Auxin regulates the initiation and radial position of plant lateral organs. *Plant Cell* **12**, 507-518.
Reinhardt, D., Pesce, E.-R., Stieger, P., Mandel, T., Baltensperger, K., Bennett, M., Traas, J., Friml, J. and Kuhlemeier, C. (2003). Regulation of phyllotaxis by polar auxin transport. *Nature* **426**, 255-260.
Reymond, M. C., Brunoud, G., Chauvet, A., Martínez-Garcia, J. F., Martin-Magniette, M. L., Monéger, F. and Scutt, C. P. (2012). A light-regulated genetic module was recruited to carpel development in Arabidopsis following a structural change to SPATULA. *Plant Cell* **24**, 2812-2825.
Ruberti, I., Sessa, G., Ciolfi, A., Possenti, M., Carabelli, M. and Morelli, G. (2012). Plant adaptation to dynamically changing environment: the shade avoidance response. *Biotechnol. Adv.* **30**, 1047-1058.
Santner, A., Calderon-Villalobos, L. I. and Estelle, M. (2009). Plant hormones are versatile chemical regulators of plant growth. *Nat. Chem. Biol.* **5**, 301-307.
Sawa, S., Ohgishi, M., Goda, H., Higuchi, K., Shimada, Y., Yoshida, S. and Koshiba, T. (2002). The HAT2 gene, a member of the HD-Zip gene family, isolated as an auxin inducible gene by DNA microarray screening, affects auxin response in Arabidopsis. *Plant J.* **32**, 1011-1022.
Schoof, H., Lenhard, M., Haecker, A., Mayer, K. F., Jürgens, G. and Laux, T. (2000). The stem cell population of Arabidopsis shoot meristems in maintained by a regulatory loop between the CLAVATA and WUSCHEL genes. *Cell* **100**, 635-644.
Sessa, G., Morelli, G. and Ruberti, I. (1993). The Athb-1 and -2 HD-Zip domains homodimerize forming complexes of different DNA binding specificities. *EMBO J.* **12**, 3507-3517.
Sessa, G., Steindler, C., Morelli, G. and Ruberti, I. (1998). The Arabidopsis Athb-8, -9 and -14 genes are members of a small gene family coding for highly related HD-ZIP proteins. *Plant Mol. Biol.* **38**, 609-622.
Smith, Z. R. and Long, J. A. (2010). Control of Arabidopsis apical-basal embryo polarity by antagonistic transcription factors. *Nature* **464**, 423-426.
Sorin, C., Salla-Martret, M., Bou-Torrent, J., Roig-Villanova, I. and Martínez-García, J. F. (2009). ATHB4, a regulator of shade avoidance, modulates hormone response in Arabidopsis seedlings. *Plant J.* **59**, 266-277.
Steindler, C., Matteucci, A., Sessa, G., Weimar, T., Ohgishi, M., Aoyama, T., Morelli, G. and Ruberti, I. (1999). Shade avoidance responses are mediated by the ATHB-2 HD-zip protein, a negative regulator of gene expression. *Development* **126**, 4235-4245.
Steinmann, T., Geldner, N., Grebe, M., Mangold, S., Jackson, C. L., Paris, S., Gälweiler, L., Palme, K. and Jürgens, G. (1999). Coordinated polar localization of auxin efflux carrier PIN1 by GNOM ARF GEF. *Science* **286**, 316-318.
Sussman, M. R., Amasino, R. M., Young, J. C., Krysan, P. J. and Austin-Phillips, S. (2000). The Arabidopsis knockout facility at the University of Wisconsin-Madison. *Plant Physiol.* **124**, 1465-1467.
Talbert, P. B., Adler, H. T., Parks, D. W. and Comai, L. (1995). The REVOLUTA gene is necessary for apical meristem development and for limiting cell divisions in the leaves and stems of Arabidopsis thaliana. *Development* **121**, 2723-2735.
Tsugeki, R., Ditengou, F. A., Sumi, Y., Teale, W., Palme, K. and Okada, K. (2009). NO VEIN mediates auxin-dependent specification and patterning in the Arabidopsis embryo, shoot, and root. *Plant Cell* **21**, 3133-3151.
Vieten, A., Vanneste, S., Wisniewska, J., Benková, E., Benjamins, R., Beeckman, T., Luschnig, C. and Friml, J. (2005). Functional redundancy of PIN proteins is accompanied by auxin-dependent cross-regulation of PIN expression. *Development* **132**, 4521-4531.
Weigel, D. and Glazebrook, J. (2002). *Arabidopsis: A Laboratory Manual.* Cold Spring Harbor, NY: Cold Spring Harbor Laboratory Press.
Weijers, D., Schlereth, A., Ehrismann, J. S., Schwank, G., Kientz, M. and Jürgens, G. (2006). Auxin triggers transient local signaling for cell specification in Arabidopsis embryogenesis. *Dev. Cell* **10**, 265-270.
Wisniewska, J., Xu, J., Seifertová, D., Brewer, P. B., Ruzicka, K., Blilou, I., Rouquié, D., Benková, E., Scheres, B. and Friml, J. (2006). Polar PIN localization directs auxin flow in plants. *Science* **312**, 883.
Zhang, Y., Mayba, O., Pfeiffer, A., Shi, H., Tepperman, J. M., Speed, T. P. and Quail, P. H. (2013). A quartet of PIF bHLH factors provides a transcriptionally centered signaling hub that regulates seedling morphogenesis through differential expression-patterning of shared target genes in Arabidopsis. *PLoS Genet.* **9**, e1003244.
Zhao, Z., Andersen, S. U., Ljung, K., Dolezal, K., Miotk, A., Schultheiss, S. J. and Lohmann, J. U. (2010). Hormonal control of the shoot stem-cell niche. *Nature* **465**, 1089-1092.
Zhao, P., Shi, D.-Q. and Yang, W.-C. (2011). Patterning the embryo in higher plants: Emerging pathways and challenges. *Front. Biol.* **6**, 3-11.
Zhong, R. and Ye, Z. H. (1999). IFL1, a gene regulating interfascicular fiber differentiation in Arabidopsis, encodes a homeodomain-leucine zipper protein. *Plant Cell* **11**, 2139-2152.
Zhong, R. and Ye, Z. H. (2004). Amphivasal vascular bundle 1, a gain-of-function mutation of the IFL1/REV gene, is associated with alterations in the polarity of leaves, stems and carpels. *Plant Cell Physiol.* **45**, 369-385.
Zúñiga-Mayo, V. M., Marsch-Martínez, N. and de Folter, S. (2012). JAIBA, a class-II HD-ZIP transcription factor involved in the regulation of meristematic activity, and important for correct gynoecium and fruit development in Arabidopsis. *Plant J.* **71**, 314-326.